China Geology 7 (2024) 12−25

China Geology

Journal homepage: http://chinageology.cgs.cn
https://www.sciencedirect.com/journal/china-geology

Potential evaluation of saline aquifers for the geological storage of carbon dioxide: A case study of saline aquifers in the Qian-5 member in northeastern Ordos Basin

Yan Li[a], Peng Li[b,*], Hong-jun Qu[b, c, d,*], Gui-wen Wang[a], Xiao-han Sun[b], Chang Ma[b], Tian-xing Yao[b]

[a] *Guoneng Jinjie Energy Co., Ltd., Shenmu* 719319, *China*
[b] *Department of Geology, Northwest University, Xi'an* 710069, *China*
[c] *Carbon Neutrality College (Yulin), Northwest University, Xi'an* 710069, *China*
[d] *National & Local Joint Engineering Research Center of Carbon Capture and Storage Technology, Xi'an* 710069, *China*

ARTICLE INFO

Article history:
Received 28 January 2023
Received in revised form 18 June 2023
Accepted 16 July 2023
Available online 1 August 2023

Keywords:
Carbon burial
Carbon neutral
CO_2 storage in saline aquifer
Distributary channel sand body
Potential evaluation
Technical control capacity
CO_2 geological storage engineering
Ordos Basin

ABSTRACT

The well-developed coal electricity generation and coal chemical industries have led to huge carbon dioxide (CO_2) emissions in the northeastern Ordos Basin. The geological storage of CO_2 in saline aquifers is an effective backup way to achieve carbon neutrality. In this case, the potential of saline aquifers for CO_2 storage serves as a critical basis for subsequent geological storage project. This study calculated the technical control capacities of CO_2 of the saline aquifers in the fifth member of the Shiqianfeng Formation (the Qian-5 member) based on the statistical analysis of the logging and the drilling and core data from more than 200 wells in the northeastern Ordos Basin, as well as the sedimentary facies, formation lithology, and saline aquifer development patterns of the Qian-5 member. The results show that (1) the reservoirs of saline aquifers in the Qian-5 member, which comprise distributary channel sand bodies of deltaic plains, feature low porosities and permeabilities; (2) The study area hosts three NNE-directed saline aquifer zones, where saline aquifers generally have a single-layer thickness of 3–8 m and a cumulative thickness of 8–24 m; (3) The saline aquifers of the Qian-5 member have a total technical control capacity of CO_2 of 119.25×10^6 t. With the largest scale and the highest technical control capacity (accounting for 61% of the total technical control capacity), the Jinjie-Yulin saline aquifer zone is an important prospect area for the geological storage of CO_2 in the saline aquifers of the Qian-5 member in the study area.

1. Introduction

Pores in sedimentary strata are largely saturated with formation water. The formation water with a total dissolved solids (TDS) content of generally 3.0–50.0 g/L is suitable for the geological storage of CO_2 in saline aquifers. Such saline aquifers are widely developed in deep sedimentary basins (Bachu S et al., 2008; Diao YJ et al., 2021). The CO_2 storage in saline aquifers refers to the storage of supercritical CO_2 in underground saline aquifers for hundreds or tens of thousands of years CO_2 through some physical and chemical mechanisms (Benson SM and Surles T, 2006; Jia LX, 2021).

Rich resources such as coal, gas, oil, salt, and uranium has highly developed in the northeastern Ordos Basin and coal chemical and coal electricity generation industries make this area China's to be largest base of coal electricity generation with huge CO_2 emissions. Therefore, there is an urgent need for carbon neutrality in this area (Liu SX et al., 2019; Ma X et al., 2021), for which an important way is the geological storage of CO_2 in saline aquifers (Ma JF et al., 2022). The northeastern Ordos Basin host thick sedimentary strata, among which the Qian-5 member, as a potential CO_2 storage stratum, has well-developed saline aquifers (He B et al., 2016). These saline aquifers are considered to be favorable for the CO_2 geological storage fot the reason of their reservoirs, caprocks, and burial depths. However, research on the geological storage of CO_2 in saline aquifers in the northeastern Ordos Basin is still at its initial stage. Despite some previous studies (Wan YY, 2012; Yang GD, 2015),

First author: *E-mail address*: 16145014@ceic.com (Yan Li).
* Corresponding author: *E-mail address*: lpenggeo@126.com (Peng Li); hongjun@nwu.edu.cn (Hong-jun Qu).

Literary editor: Xi-jie Chen
doi:10.31035/cg2023045
2096-5192/© 2024 China Geology Editorial Office.

there is an absence of studies on the development and distribution patterns and the potential for CO_2 storage of the saline aquifers in the Qian-5 member in this area, leading to a lack of macroscopic, systematic understanding in this regard. It has practical significance to study the development and distribution patterns of the saline aquifers and to evaluate the potential of the saline aquifers for the CO_2 geological storage. This study relies on the whole-process demonstration project of the post-burning capture and oil-displacement-based CO_2 storage of a coal power plant in the Jinjie Energy Co., Ltd. under CHN Energy (also referred to as the Demonstration Project). This project has been in operation since June 2021, and its capture equipment with a design annual capture capacity of 150000 tons is located in Jinjie Town, Shenmu City. Given the limited demand for chemical utilization and oil displacement of CO_2, this study intends to directly implement the short-distance storage of CO_2 captured from this project into moderately deep saline aquifers.

Bachu S (2000) proposed that the geological storage of CO_2 in basins should consider the tectonic setting, geothermal regime, hydrodynamic characteristics, oil and gas potential, and exploration intensity of the basins, as well as economic, political, and social factors. Bachu S (2003), by assigning different weight coefficients to 15 siting evaluation criteria, evaluated the suitability of 12 basins in Canada for the geological storage of CO_2. The weighting method has become a commonly used method for the site selection of CO_2 storage in saline aquifers. Chinese researchers also built some assessment systems for site selection in sedimentary basins. Li FC et al. (2014) developed four major evaluation indicators, namely geological safety, storage scale, social and environmental risks, and economic suitability, which can be divided into 28 secondary indicators. Song TJ et al. (2017) evaluated the suitability of 33 second-order tectonic units in the Songliao Basin through the grey relational analysis from the perspective of storage scale, storage safety, social and environmental risks, and economic suitability. Guo JQ (2015) divided the potential and suitability evaluation of the geological storage of CO_2 in China into regional, basin, target, site, and injection stages and defined the evaluation criteria of the five stages. Sun TM et al. (2021) also divided the potential and suitability evaluation of the geological storage of CO_2 into the same five stages and roughly evaluated the storage potential of CO_2 in China at regional and basin levels. Cao ML and Chen JP (2022) proposed that the feasibility evaluation of the geological site selection for CO_2 storage in deep saline aquifers should be conducted from seven aspects, namely, geotectonic setting, volume, reservoirs, caprocks, structures, regional stability, and hydrology.

The potential for CO_2 storage refers to the multiple level storage capacities at different units under the influence of technical and economic factors. This study focuses on target-level CO_2 storage potential. In other words, surrounding stationary carbon emission sources, this study evaluates the potential for CO_2 storage at the level of first- and second-order tectonic units in the basin (Sun TM et al., 2021). It conducted a statistical analysis of the drilling and logging data from 239 wells in the northeastern Ordos Basin, together with the analytical and testing data of cores from partial wells. Furthermore, based on logging interpretation, it determined the development patterns of the sedimentary facies in the Qian-5 member, alongside the distribution patterns and porosities of the saline aquifers in the member. Based on these, this study evaluated the potential of saline aquifers in the Qian-5 member for the geological storage of CO_2 in the northeastern Ordos Basin by calculating the technical control capacities of CO_2 in the saline aquifers. The technical control capacity is the storage capacity further calculated based on set technical conditions and controlled geological potential, which refers to the theoretical storage capacity estimated by assuming that pore spaces in reservoirs of favorable targets or their internal geological units are filled with CO_2 to the maximum degree. The controlled geological potential can be obtained through the pre-exploration of the geological storage of CO_2 in saline aquifers or based on the existing exploration density and geological data that meet the requirements of the pre-exploration stage (Diao YJ et al., 2022).

2. Regional geological setting

2.1. Structural characteristics of the northeastern Ordos Basin

As China's second-largest onshore sedimentary basin, the Ordos Basin is an intracratonic depression basin formed by the superimposition of Paleozoic platforms, platform-margin depressions, and Meso-Cenozoic intra-platform depressions. Featuring relatively stable structures and low geotemperature gradients, the Ordos Basin is a low-temperature basin. Moreover, this basin is composed primarily of six first-order tectonic units, namely, the Yimeng uplift, the Yishan slope, the Jinxi fault-fold belt, the Tianhuan depression, the Weibei uplift, and the western-margin tectonics belt (Fig. 1a; Liu CY et al., 2006).

The study area, located in the northeast Yishan slope, is a slope structure higher in the east and lower in the west. It has simple internal structures, with formation dip angles of 1° or less. It hosts a low-amplitude, nose-shaped structure and relatively undeveloped faults, with almost the absence of magmatic and metamorphic activities. At burial depths of 1350–2700 m, the study area has temperature and pressure conditions surpassing those required for supercritical CO_2, thus meeting the requirements for safe CO_2 storage (Fig. 1b).

2.2. Strata in the northeastern Ordos Basin and lithology of the Qian-5 member

The Ordos Basin 's basement where the northeastern Ordos Basin is positioned consists of Archean and Lower Proterozoic metamorphic rocks. The sedimentary caprocks in the area consist of strata of all geological eras except for the Lower Carboniferous, Devonian, and Silurian. The Upper Paleozoic strata in the northeastern Ordos Basin consist of

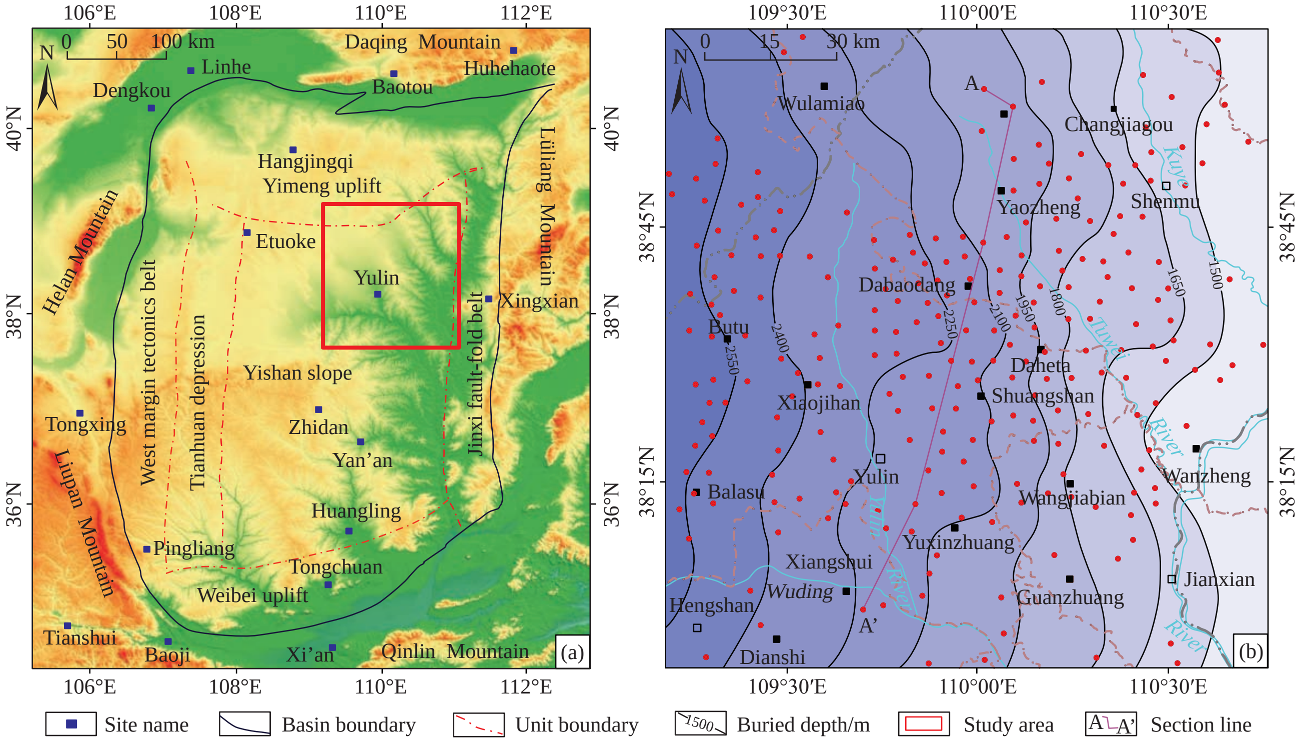

Fig. 1. Regional tectonic location (a) and burial depths of the top surface of the Qian-5 member (b) in the northeastern Ordos Basin.

coal measures strata with a thickness of about 1000 m and considerably thick fluvial-lacustrine clastics. The Upper Permian Shiqianfeng Formation, which has an average thickness of 280 m, can be divided into five members from top to bottom. Among these members, the Qian-5 member in the lower part holds stable saline aquifers, above which is the Triassic Liujiagou Formation with a thickness of about 400 m.

The Qian-5 member in the Ordos Basin comprises interbeds consisting of brownish-red sandstones and purplish-red mudstones, with sedimentary facies dominated by the sedimentary system of lacustrine-braided river deltas (Guo YQ et al., 2019). In addition, the Qian-5 member in the northeastern Ordos Basin mainly shows the braided river deltaic plain subfacies (Wang RG, 2016; Zhang DF et al., 2021).

2.3. Reservoir-caprock assemblages of saline aquifers in the Qian-5 member

The outcrop in the north of study area was surveyed, which indicate that Qian-5 member is promising reservoir for CO_2 geological storage. The reservoir of the Qian5 member is mainly characterized by thick medium- to coarse-grained sandstones with conglomerate layers (Fig. 2). Due to weak diagenesis or weathering, the lithology is loose and the reservoir property (porosity and permeability) generally high (unpublished data).

The Qian-5 member of the Upper Permian Shiqianfeng Formation in the northeastern Ordos Basin, which has an average thickness of about 60 m, hosts relatively stable saline aquifers. The Qian-4 to Qian-1 members above the Qian-5 member host mudstone and silty mudstone caprocks with a cumulative thickness greater than 150 m. These thick caprocks show a continuous distribution pattern, a high breakthrough pressure, and high sealing performance (Ma DY, 2021). Above these strata is the Lower Triassic Liujiagou Formation, which has a thickness greater than 400 m and is composed primarily of mudstones and silty mudstones. These mudstone caprocks are extremely thick, with burial depths of 1500–2500 m. Therefore, the Qian-5 member is a favorable potential geological storage body of CO_2 (Fig. 3).

3. Sedimentary facies and reservoir characteristics of the Qian-5 member

3.1. Sedimentary facies in the Qian-5 member

The sedimentary facies in the Qian-5 member in the study area are dominated by the braided river deltaic plain subfacies, which can be divided into distributary channel and interdistributary bay microfacies. The reservoirs of saline aquifers in this member consist primarily of distributary channel sand bodies. The study area hosts three NNE-orientated distributary channels with a direction of SW and widths of generally 15–25 km (Fig. 4).

3.2. Reservoirs in the Qian-5 member

3.2.1. Petrological characteristics of reservoirs in the Qian-5 member

As shown by the microscopic identification data of 400 casting thin sections, the sandstone reservoirs in the Qian-5 member feature low textural maturity, low mineral maturity, and relatively coarse grains. They are composed primarily of medium- to coarse-grained sandstones dominated by lithic

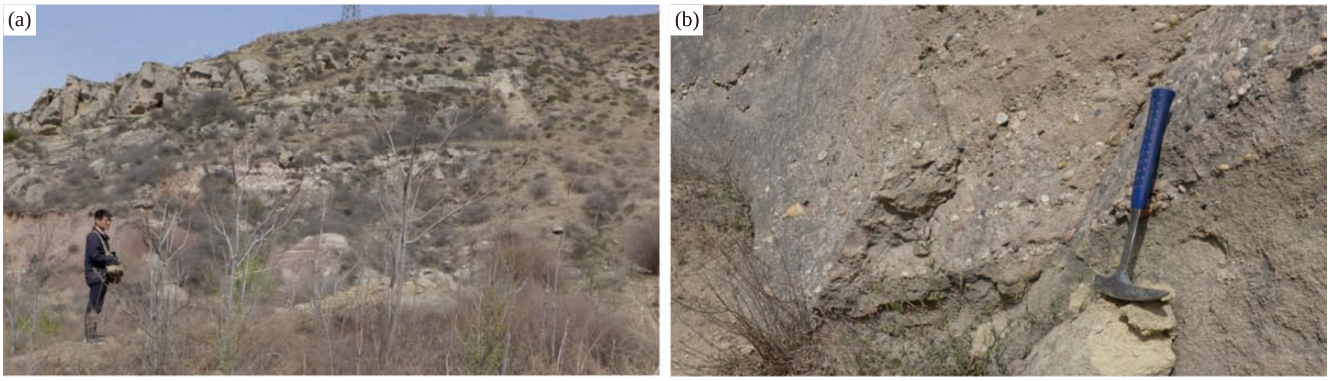

Fig. 2. Outcrop characteristics of macroscopic reservoir (a) and petrology (b) of the Qian-5 member in the northeastern Ordos Basin.

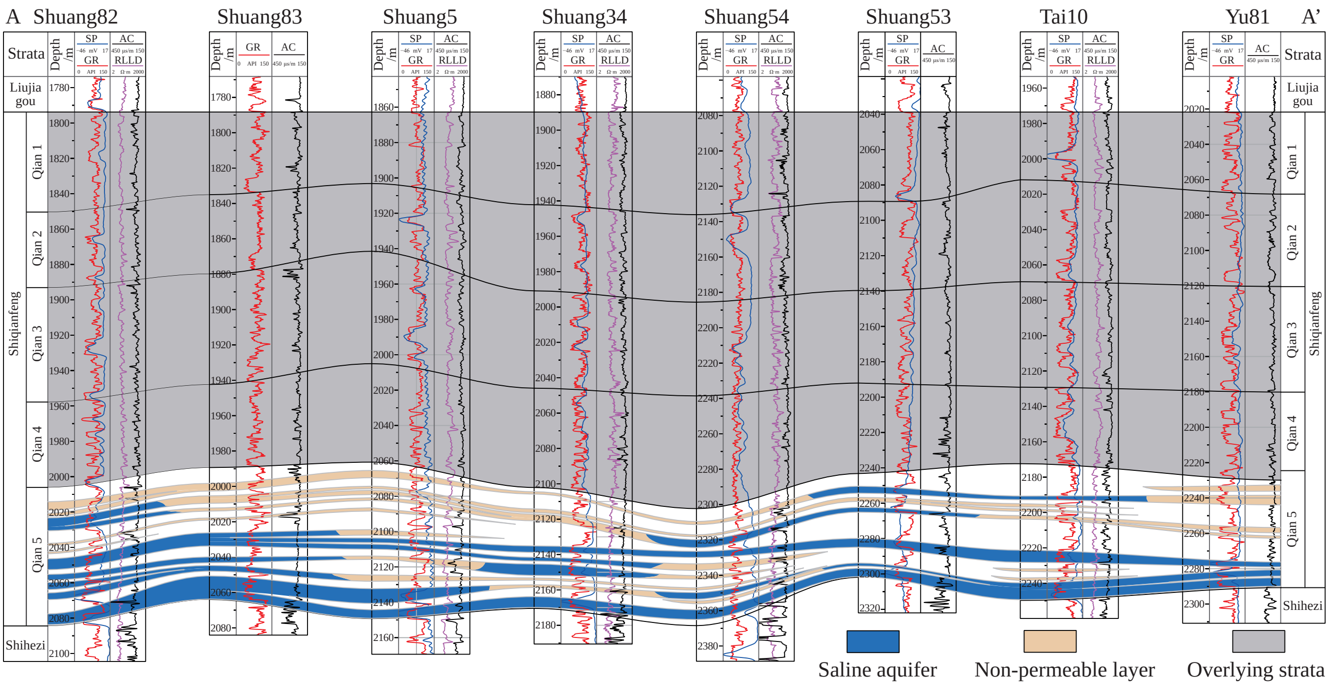

Fig. 3. Comprison of the reservoir-caprock assemblages of saline aquifers in the Qian-5 member in the northeastern Ordos Basin (section position: A-A' in Fig. 1).

feldspar sandstones and feldspathic lithic sandstones, followed by feldspar sandstones, lithic sandstones, and small amounts of lithic and feldspathic quartz sandstones.

3.2.2. Microscopic pore structures of reservoirs in the Qian-5 member

Pores in the reservoirs of the Qian-5 member mainly include residual intergranular pores (Fig. 5a), followed by feldspar dissolved pores (Fig. 5b), lithic dissolved pores, intercrystalline pores, and gelatinous tuffaceous matrix contraction fractures (Fig. 6).

3.2.3. Physical properties of reservoirs in the Qian-5 member

The reservoirs of saline aquifers in the Qian-5 member have porosities of mainly 5–12%, peaking at 7–11% and averaging 8.38%, and samples with such porosities accounted for about 50% of the total samples (Fig. 7). They have permeabilities of 0.1–10 (10^{-3} μm^2), and samples with such permeabilities accounted for about 70% of the total samples. Therefore, the reservoirs of saline aquifers are mostly low-porosity and low-permeability.

4. Distribution patterns of saline aquifers in the Qian-5 member

4.1. Identification of saline aquifers based on log interpretation

The wells of the study area were derived from natural gas exploration wells, which include complete conventional logging curves in the Qian-5 member. The saline aquifers in this member can be identified through logging interpretation. In the sandstone-mudstone sections, the different TDS contents between formation water and mud lead to anomalous spontaneous potential (SP) of saline aquifers, and the study area generally show negative SP anomalies. Owing to the intrusion of mud filtrate, the resistivity log curves of deep and shallow parts are not coincident, such as dual laterolog

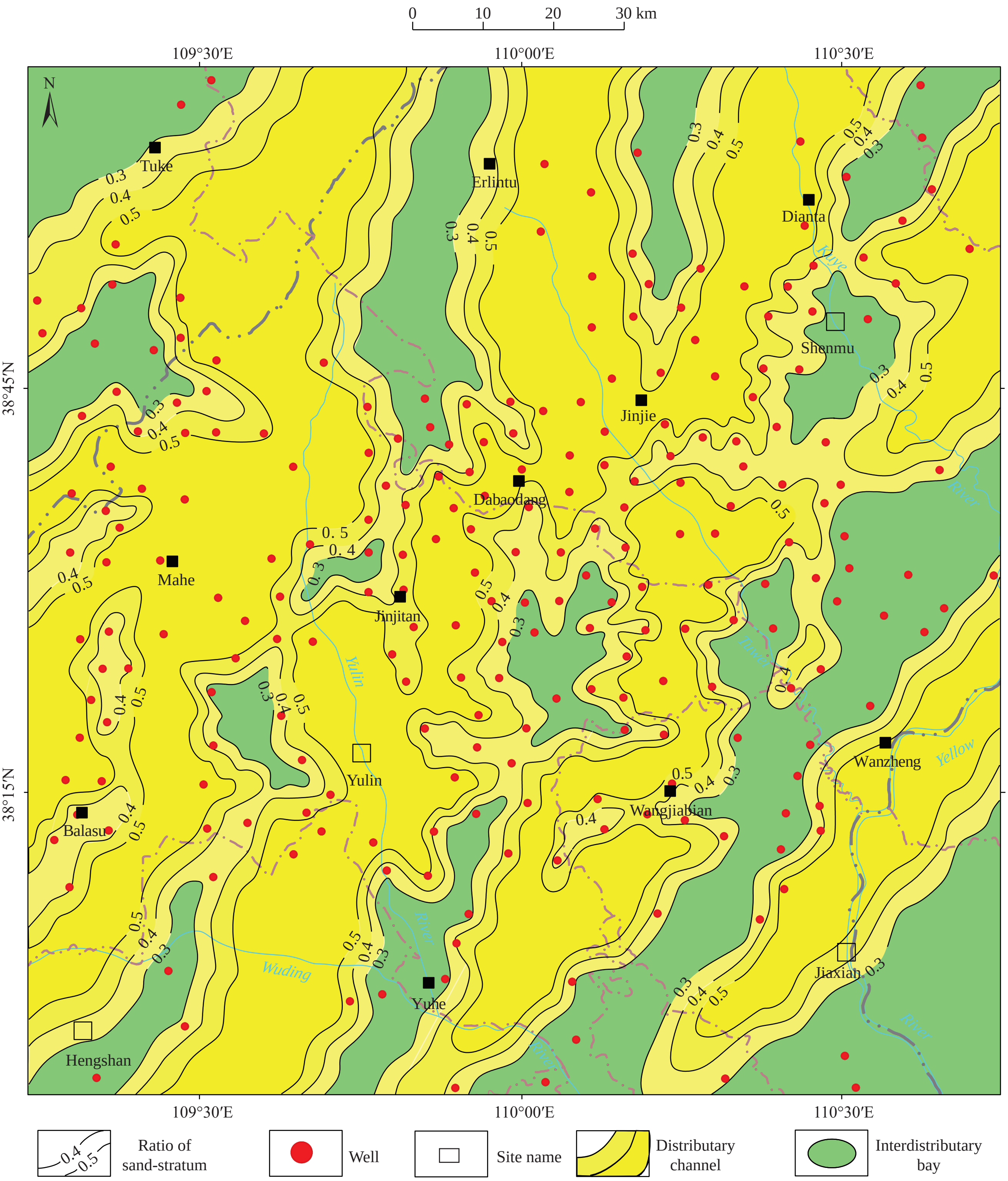

Fig. 4. Plane view of the sedimentary facies in the Qian-5 member in the northeastern Ordos Basin.

resistivity curves RLLD (deep investigate double lateral resistivity log) and RLLS (shallow investigate double lateral resistivity log) and array induction log curves RT10, RT20, RT30, RT60, and RT90. However, the differences between these curves depend on the relative TDS contents between mud filtrate and formation water, leading to insignificant curve characteristics in some wells. Therefore, these resistivity log curves can be used as a reference in the identification of saline aquifers (Nan D et al., 2022). Other log curves, such as the acoustic interval transit time (AC), density (DEN), and neutron (CNL) curves, can be used to quantitatively calculate the porosities of saline aquifers. Generally, AC curve-derived porosity of more than 5% indicates saline aquifers suitable for CO_2 storage (Fig. 8). Given engineering factors, the lower thickness limit of saline aquifers was set at 3 m in this study. Based on the discussion

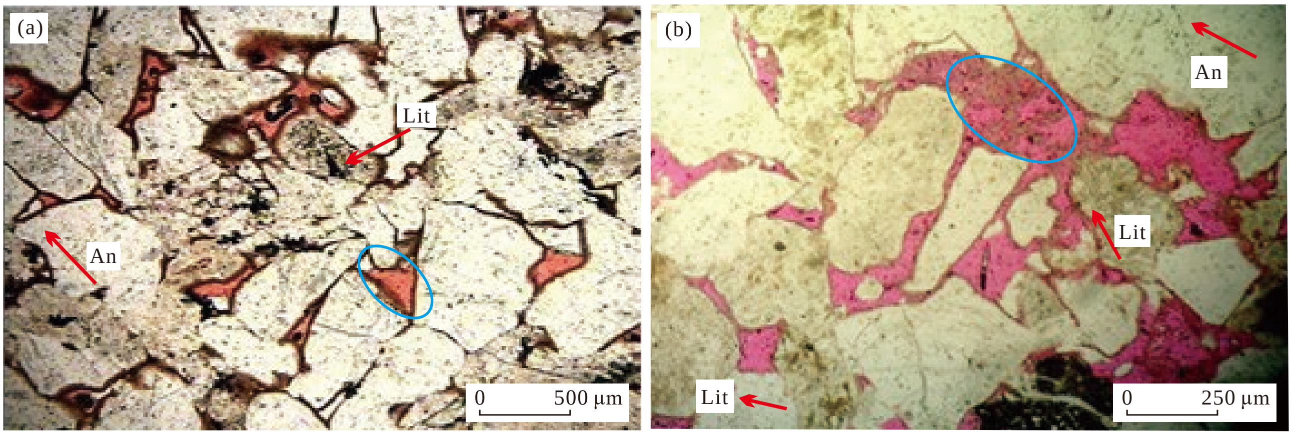

Fig. 5. Intergranular pores (a) and feldspar dissolved pores (b) in reservoirs of the Qian-5 member. (a)–well Shen-8, ×5, plane-polarized light; (b)–well Yu-26, ×5, plane-polarized light. Lit refers to lithic fragment and An refers to feldspar minerals.

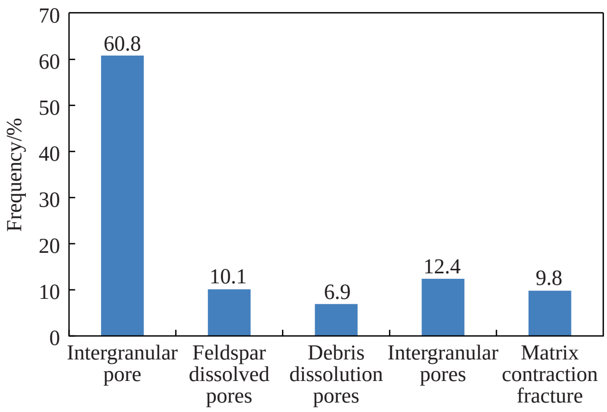

Fig. 6. Distribution frequencies of various pores in reservoirs of the Qian-5 member in the northeastern Ordos Basin (320 samples).

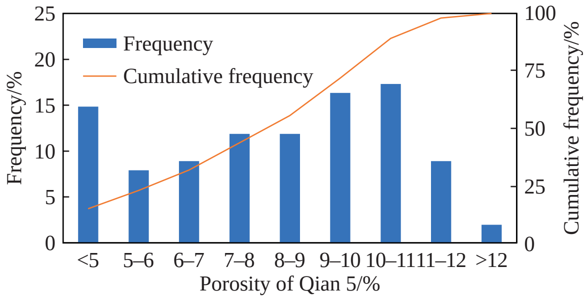

Fig. 7. Porosity distribution frequencies of reservoirs in the Qian-5 member in the northeastern Ordos Basin.

mentioned above, this study identified saline aquifers at 239 wells in the Qian-5 member in the study area based on log interpretation.

4.2. Development of saline aquifers in the Qian-5 member

As shown by the identification results based on logging interpretation, the saline aquifers in the Qian-5 member of the northeastern Ordos Basin have single-layer thicknesses of 3–17.8 m (average: 5.7 m), and those with single-layer thicknesses of 3–5 m account for about 50% of all saline aquifers identified (Fig. 8a). The saline aquifers have single-

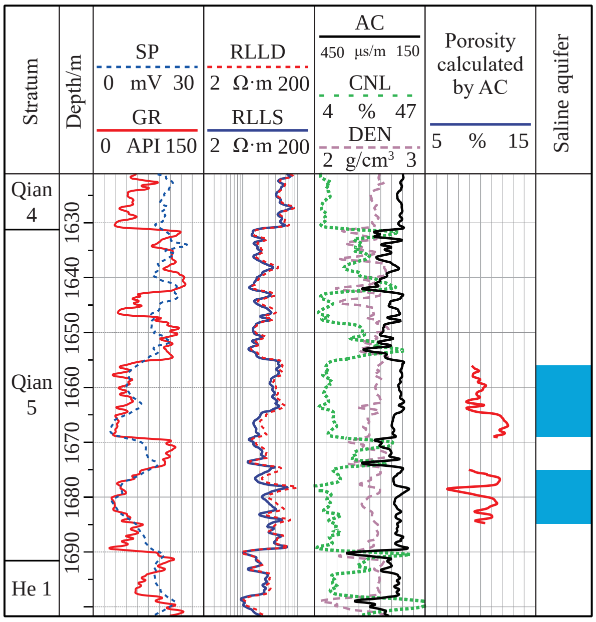

Fig. 8. Identification of saline aquifers based on log interpretation (well Shen-8).

well cumulative thicknesses of 0–40.6 m (average: 15.6 m). The Qian-5 member hosts 2–4 major saline aquifers, with cumulative thicknesses of primarily 8–24 m (Fig. 8b).

4.3. Distribution patterns of saline aquifers in the Qian-5 member

The distributions of saline aquifers in the study area are mainly influenced by distributary channel sand bodies. Relatively thick saline aquifer zones are continuously distributed along the major channel sand bodies, extending primarily from northeast to southwest. Three saline aquifer zones occur in three major channels in northern Jiaxian, Yulin-Jinjie, and Mahe in Yuyang. These saline aquifer zones generally have thicknesses of about 20 m or above and widths of 15–25 km, thinning gradually toward the channel edges. Those saline aquifers have cumulative thicknesses less than 8 m generally in interdistributary bays (Fig. 9).

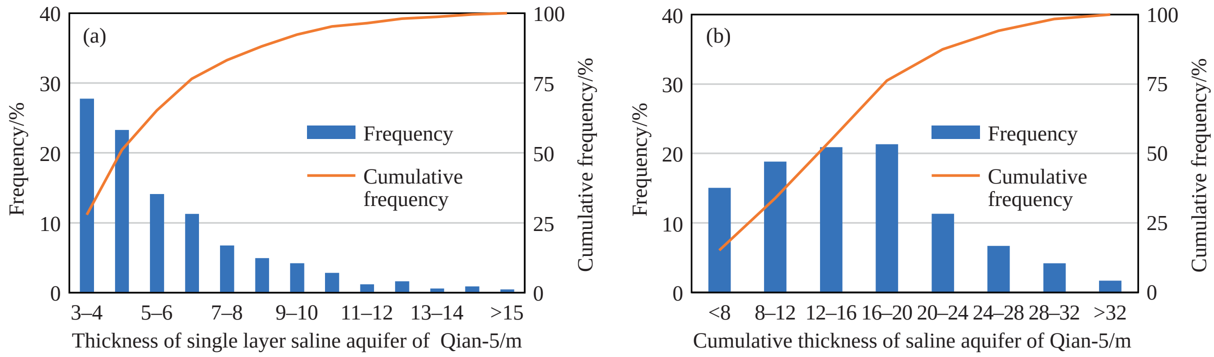

Fig. 9. Thicknesses of saline aquifers in the Qian-5 member in the northeastern Ordos Basin. (a)–frequencies of single-layer thickness; (b)–frequencies of single-well cumulative thickness.

This study further analyzed the development of the saline aquifers based on the EW-directed well sections in the northern portion of the study area (Fig. 10). As shown by the well sections, the saline aquifers in the Qian-5 member have a higher scale and high connectivity than those in the Qian-4 member above. However, the presence of some impermeable mudstone interlayers or tight sandstones increases the heterogeneity of reservoirs in the saline aquifers (Fig. 11).

4.4. Hydrogeological characteristics of saline aquifers

Based on different aquifer media, the Ordos Basin contains five aquifer systems, namely the Precambrian bedrock fracture aquifer system, the Cambrian-Ordovician carbonate karst aquifer system, the Cretaceous clastic fissure-pore aquifer system, the aquifer system of Carboniferous-Jurassic clastic fissures and their overlying loose-layer pores, and the aquifer system of Cenozoic faulted basin pores (Hou GC et al., 2008). The aquifer systems in the upper part are recharged *via* the infiltration of meteoric water and surface water. They finally discharge from the base level of erosion such as the rivers and lakes, forming shallow runoff opening zone (Fig. 12). In contrast, the aquifer systems in the lower part are deep closed runoff retention zones. For the study area, its main body hosts the aquifer system of Carboniferous-Jurassic clastic fissures and their overlying loose-layer pores, while its northern part exhibits the Cretaceous clastic fissure-pore aquifer system locally. The shallow runoff opening zones of the former and latter aquifer systems have maximum circulation depths of up to 300 m and 1000 m, respectively. These shallow runoff opening zones have a hydrochemical type of HCO_3, which shifts to the CI type below the bottom boundary of the weathering zone as the TDS content of formation water increases with the depth.

The entire Qian-5 member in the study area is positioned in the deep closed retention zone. Above this member is the Liujiagou Formation, which serves as an aquiclude with a stable thickness. As a result, except for oil and natural gas wells, there is almost no pathways for water exchange between the Qian-5 member and the shallow runoff opening zone. Accordingly, the Qian-5 member is long in a retention or closed state, and large quantities of salts in the member are dissolved, increasing the TDS content of groundwater and making it unsuitable for living or production. As shown by the formation water samples from the Shiqianfeng Formation, the groundwater in the formation has a hydrochemical type of Cl-Ca·Na, with a TDS content of 31212.34 mg/L. The anions in the groundwater are dominated by Cl^-, which has a concentration of 17935.68 mg/L and accounts for 89.87% of the total anions, respectively. Cl^- is followed by SO_4^{2-}, which has a concentration of 1944.69 mg/L and accounts for 9.74% of the total anions. The main cations in the groundwater include Ca^{2+} and Na^+, which have concentrations of 6445.25 mg/L and 4558 mg/L and account for 57.30% and 40.52% of the total cations, respectively (Diao YJ, 2017).

5. Assessing the potential of saline aquifers in the Qian-5 member for the geological storage of CO_2

5.1. CO_2 storage mechanism

The main CO_2 storage mechanism of the Qian-5 member is the lithologic trap capture, during which the injected CO_2 migrates upward and displaces formation water mainly along high-seepage pathways such as distributary channel sand bodies. This storage mechanism controls the distribution of CO_2 plume, thus further controlling the influencing ranges of the dissolution capture, irreducible gas capture, and mineralization capture of CO_2. Generally, the lithologic trap capture of CO_2 dominates during the operation of CO_2 storage projects (Diao YJ, 2021).

The dissolution capture of CO_2 usually plays a secondary role during the operation of CO_2 storage projects. The CO_2 dissolution, which occurs at the interface between CO_2 and formation water on a temporal scale of tens to thousands of years (Lindeberg E and Wessel-Berg D, 1997), primarily depends on the formation pressure, temperature, and hydrochemical parameters. The CO_2 dissolution in formation water increases the density of formation water by about 1%. Moreover, CO_2 disperses and settles downward in saline aquifers, further enhancing the CO_2 storage capacity of reservoirs (Bachu S and Adams J, 2003; Kumar A et al., 2004). However, this convection progress is potentially hindered by the presence of interlayers in reservoirs of the Qian-5 member, thus further affecting the potential for the dissolution capture of CO_2 on a short temporal scale.

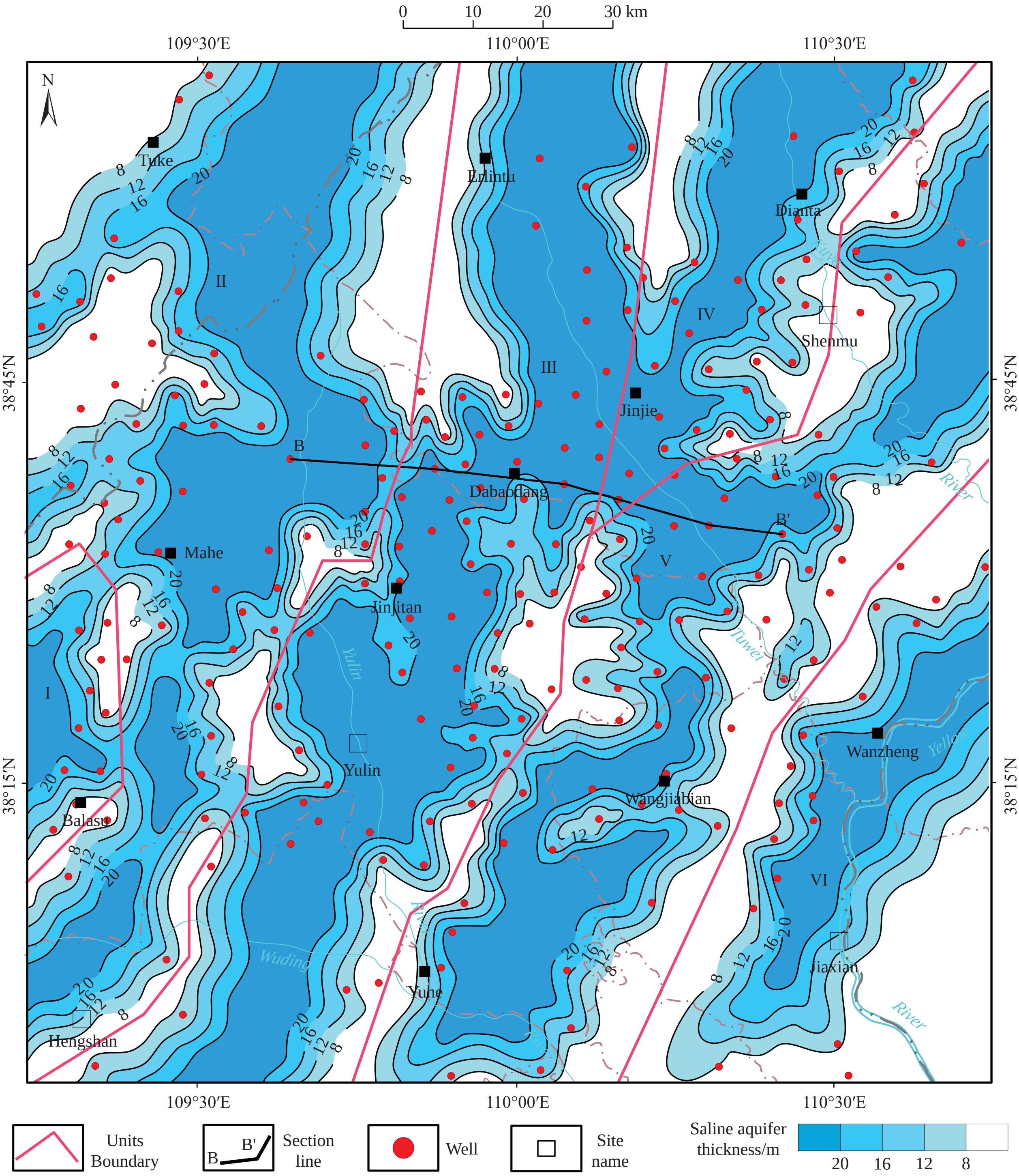

Fig. 10. Distributions of saline aquifers in the Qian-5 member in the northeastern Ordos Basin.

The irreducible gas capture of CO_2 is as follows: as non-wetting supercritical CO_2 is injected into reservoirs, part of CO_2 is captured as discontinuous residual gas due to hysteresis of relative permeability when wetting formation water at the back end of CO_2 plume retreats, absorbs CO_2, and re-saturates pores. This capture process, spanning tens to thousands of years, depends primarily on displacement pressure and wettability, and its storage capacity is mainly dictated by the influencing range and pore diameter of the CO_2 plume (Bachu S et al., 2008).

The mineralization capture of CO_2 is based on dissolution capture. The saline aquifers of the Qian-5 member in the study area have high Na^+ and Ca^{2+} contents (Table 1). The injection of CO_2 can produce CO_3^{2-}, which can be further ionized into H^+ and HCO^{3-}. Among them, H^+ can significantly enhance the acidity of formation water, further leading to the dissolution of lithics and feldspar minerals in the Qian-5 member and the release of cations such as K^+, Na^+, Ca^{2+}, and Mg^{2+}. The released cations combine with CO_3^{2-}, forming carbon-fixing minerals like dawsonite, calcite, dolomite, and

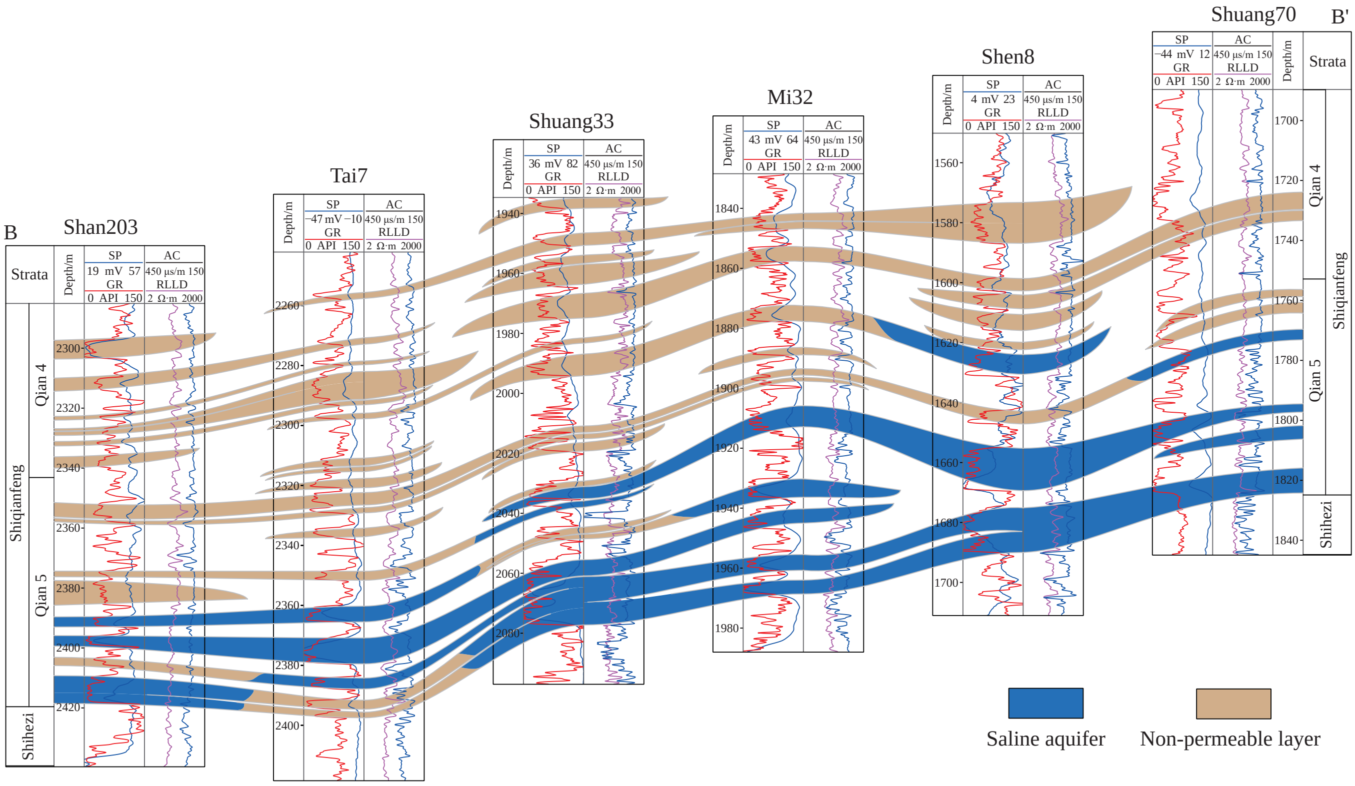

Fig. 11. Well sections of EW-directed saline aquifers in the northern part of northeastern Ordos Basin (section location: B-B’ in Fig. 10).

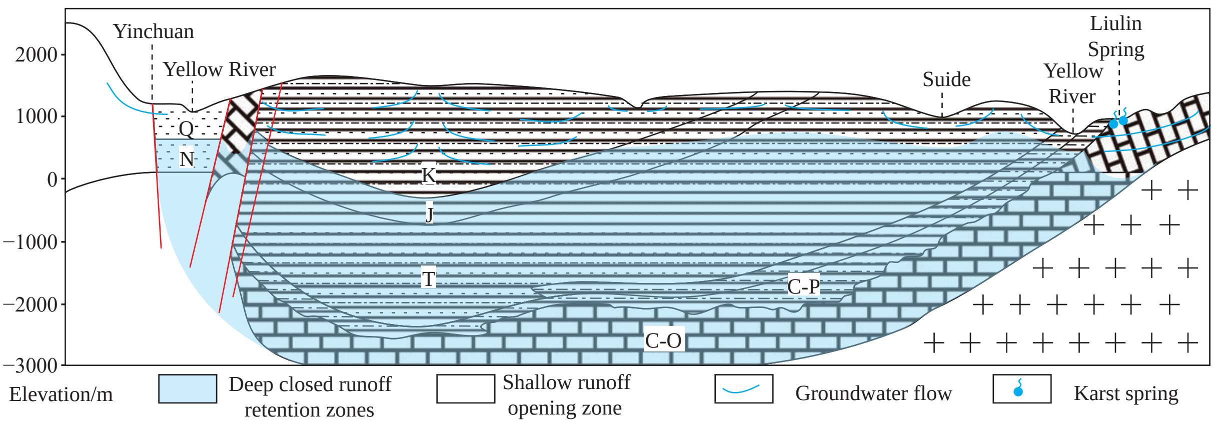

Fig. 12. Structural section of the groundwater system in the Ordos Basin (modified after Hou GC et al., 2008).

Table 1. Quality of formation water in the Shiqianfeng Formation (after Diao YJ, 2017).

Test item	K	Na^+	Ca^{2+}	Mg^{2+}	TFe	HCO_3^-	CO_3^{2-}	Cl^-
Value/mg·L^{-1}	24.52	4558	6445.25	201.29	18.97	63.06	0	17935.68
Test item	SO_4^{2-}	F^-	NO− 3	TDS	Soluble SiO_2	Free CO_2	pH	Total hardness
Value/mg·L^{-1}	1944.69	2.5	15	31212.34	3.38	110.14	4.64	10950.06

ferrodolomite. Therefore, the Qian-5 member has high potential for mineralization capture. However, the mineralization capture of CO_2 requires long-term full contact between CO_2 solution and reservoir rocks on a temporal scale usually greater than a thousand years. Therefore, the contribution of mineralization capture to CO_2 storage capacity is almost negligible during the operation of the project (Bachu S et al., 2008; Yang YZ et al., 2009).

Overall, the relative CO_2 storage capacities of the four storage mechanisms mentioned above change with the temporal scale; however, the actual CO_2 storage capacity of the project is primarily related to the trap capture mechanism.

5.2. Calculation method for technical control capacity

Based on the CO_2 capture mechanisms, saline aquifers’ geological storage capacity of CO_2 can be calculated using the structural, dissolution, bound-gas, and mineral capture mechanism methods. The structural capture mechanism method, also known as the volumetric method, is primarily based on the actual available space for underground storage (Bachu S et al., 2008; Cao ML and Chen JP, 2022). In the early exploration stage of CO_2 storage projects, there are usually no available data on reservoir cores or formation water tests, thus lacking the experiment and test parameters necessary for the dissolution, irreducible gas capture, and mineralization capture mechanism methods. By contrast, the volumetric method requires fewer parameters. The northeastern Ordos Basin is a natural gas exploration area. Accordingly, owing to the abundant drilling and log data and high well amounts of the Qian-5 member in the basin, log interpretation allows the identification of saline aquifers and reservoir porosities, thus providing reliable data for determining technical control capacities. The volumetric method can be applied to the early exploration stage of CO_2 storage projects in basins that have experienced oil and gas development to some extent.

It is assumed that reservoirs have open boundaries in the volumetric method. Under this assumption, the CO_2 injected into the reservoirs will drive groundwater in the evaluation units into surrounding hydrogeological units and fill all pores, without significantly increasing the fluid pressure of boundary strata (Popova OH et al., 2012). The equation of the volumetric method is as follows:

$$M_{CO_{2t}} = A \cdot h_g \cdot \phi \cdot \rho_{CO_{2r}} \cdot E(\text{USDOE}, 2006) \quad (1)$$

where $M_{CO_{2t}}$ is the potential storage capacity of CO_2, Kg; A is the total area of the area to be evaluated, m^2; h_g is the effective thickness of reservoirs in the area to be evaluated, m; ϕ is the average porosity of reservoirs in the area to be evaluated, %; $\rho_{CO_{2r}}$ is the density of CO_2 under formation conditions, $kg \cdot m^{-3}$; E is the storage efficiency factor, dimensionless. In actual geological conditions, CO_2 storage is feasible only when saline aquifers have a certain thickness and injectability. Therefore, the effective units for the geological storage of CO_2 are determined by setting the lower limits of the single-layer thickness and porosity of saline aquifers. In addition, it is impossible for CO_2 to fill all pores due to limited injection pressure and the influence of other factors such as buoyancy, capillary force, and reservoir heterogeneity. Therefore, storage efficiency factor E is used to help quantitatively evaluate the effects of the above factors on the storage capacity.

5.3. Determination of calculation units

The water bodies in the Qian-5 member of the study area are retained water. The connectivity and scales of saline aquifers are controlled by permeable sand bodies. Given that the non-permeable mudstones in interdistributary bays act as lateral aquicludes, the saline aquifers in the study area were divided into six calculation units according to the mudstones in the interdistributary bays (Fig. 10). Each unit can be considered a relatively independent hydrogeological unit. Specifically, saline aquifers within the calculation units exhibit high connectivity in the extension direction (NNE) of permeable sand bodies, while those between different calculation units show poor connectivity. The determination of these calculation units can avoid the significantly different densities of supercritical CO_2 caused by the differences between the formation temperatures and pressures of different zones, thus improving the calculation accuracy. From west to east, the six calculation units covered areas of 396 km^2, 4140 km^2, 4191 km^2, 1369 km^2, 3368 km^2, and 1507 km^2, respectively and contained 6, 43, 68, 23, 50, and 12 wells, which can almost control the distributions of saline aquifers.

5.4. Parameters for calculating the technical control capacity

5.4.1. Effective thicknesses of saline aquifers

There are no unified criteria for the minimum effective thicknesses of saline aquifers suitable for CO_2 injection. Since it is difficult and costly to conduct operations such as the perforation and fracturing of saline aquifers with thicknesses less than 3 m in actual engineering, the lower limit of the single-layer thickness of saline aquifers was set at 3 m in this study. As shown by the occurrence patterns of sand bodies in the Qian-5 member, saline aquifers with cumulative thicknesses less than 8 m are primarily located in interdistributary bays, and their reservoirs feature poor connectivity and low porosities. Therefore, the lower limit of the single-well cumulative thickness of saline aquifers was set at 8 m. Based on this lower limit, the six calculation units from west to east had average effective cumulative thicknesses of 16.88 m, 16.27 m, 19.66 m, 16.67 m, 16.01 m, and 14.94 m, respectively.

5.4.2. Effective porosities

Reservoirs with low porosities usually exhibit poor storage performance, complex pore structures, and low seepage capacity. The injection of CO_2 into these reservoirs will cause a rapid increase in injection pressure, threatening injection safety. Therefore, the lower porosity limit of reservoirs suitable for CO_2 injection is generally set at 5% in the siting for CO_2 storage (Wang ZJ et al., 2022; Diao YJ et al., 2021).

The AC logging in the study area generally covers the whole well intervals, including the saline aquifers of the Qian-5 member. The AC curves are commonly used for interpreting the porosities of saline aquifers. Moreover, based on the log interpretation results of the Qian-5 member, this study developed the AC *vs.* porosity cross plots (Fig. 13), the linear regression of which revealed that the porosity of reservoirs in the Qian-5 member is φ (%) = 0.2452 AC − 45.335.

As shown by the planar distribution of the porosity (Fig. 14), the high-porosity zones correspond to the major channel sand bodies to a certain extent. Specifically, they are roughly distributed along the extension direction of distributary channel sand bodies, and zones with porosities greater than

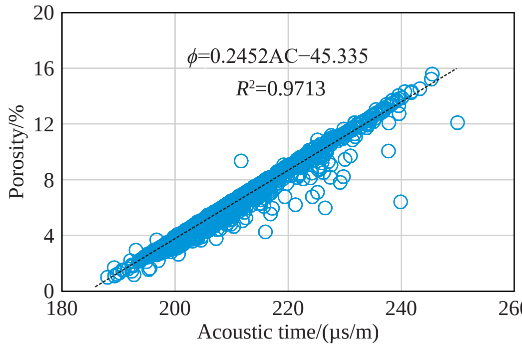

Fig. 13. Acoustic interval transit time *vs.* porosity of the northeastern Ordos Basin.

8% are distributed intermittently along major channels. The six calculation units had average porosities of 8.84%, 8.56%, 8.61%, 8.78%, 7.96%, and 6.55%, respectively.

5.4.3. Density of supercritical CO_2

CO_2 is in the supercritical state under the temperature and pressure conditions of the Qian-5 member throughout the study area. This supercritical state prevents the injected CO_2 from migrating to the top of saline aquifers to form a vapor phase zone, thus avoiding significant gradients of CO_2 density, which affect the calculation accuracy of the volumetric method. The density of supercritical CO_2 was calculated primarily based on the temperatures and pressures of the saline aquifers in the middle parts of the calculation units. The formation pressure coefficient of the study area was set at 0.765 —the average of the maximum and minimum pressure coefficients in the eastern Ordos Basin (Liu Z et al., 2012). By referencing the geothermal gradient distributions in the Ordos Basin (Ren ZL et al., 2007), the six calculation units from west to east had geothermal gradients of 2.75 °C/100 m, 2.8 °C/100 m, 2.85 °C/100 m, 2.85 °C/100 m, 2.95 °C/100 m, and 2.95 °C/100 m, respectively (Table 2).

5.4.4. Effective coefficient

The effective coefficient E is the ratio of the actual volume of injected CO_2 to the pore space (Bachu S, 2015). It can be calculated using the following equation:

$$E = E_{An/At} \cdot E_{hn/hg} \cdot E_{\phi e/\phi tot} \cdot E_v \cdot E_d \quad (2)$$

where $E_{An/At}$ is the effective area coefficient, which refers to the ratio of the effective area suitable for CO_2 storage to the total area; $E_{hn/hg}$ is the effective thickness coefficient, which refers to the thickness corresponding to the minimum porosity and permeability required for CO_2 injection; $E_{\varphi e/\varphi tot}$ is the effective porosity coefficient, which refers to the ratio of the effective porosity to the total volume, such as interconnected porosity; E_v is the effective volume displacement coefficient, which refers to the contact volume of CO_2 plume within a certain range around the CO_2 injection wells and can be determined by reservoir heterogeneity, injection pressure, and density gradient; E_d is the microscopic displacement coefficient, which refers to the proportion of the microscopic volume of the in situ pore fluids that are free from capillary force and can be displaced by injected CO_2 (Goodman A et al., 2011).

As calculated based on the basic data from oil and gas reservoirs in basins in North America using the Monte Carlo method, the values of the aforementioned parameters are shown in Table 3. The effective coefficient E under three probabilities was calculated at 1.2% (P_{10}), 2.4% (P_{50}), and 4.1% (P_{90}) (Table 3). Compared with oil and gas reservoirs in North America, the reservoirs in the Qian-5 member exhibit inferior physical properties and strong heterogeneity. Given this, E was set at 1.2% in this study.

5.5. Evaluation of the potential of the saline aquifers in the Qian-5 member for the geological storage of CO_2

As indicated by the calculation results of the volumetric method, the six calculation units from west to east had technical control capacities of 3.77 × 10^6 t, 35.62 × 10^6 t, 41.78 × 10^6 t, 10.53 × 10^6 t, 21.03 × 10^6 t, and 6.52 × 10^6 t, respectively. Therefore, the technical control capacity of the study area totals 119.25 × 10^6 t (Table 4). The Yulin-Jinjie saline aquifer zone, which covers three calculation units Ⅲ, Ⅳ, and Ⅴ adjacent to stationary carbon emission sources such as Yulin-Jinjie, has a cumulative technical control capacity of 73.34 × 10^6 t, which accounts for 61% of the total capacity of the study area. Therefore, the Yulin-Jinjie saline aquifer zone is an important prospect area for CO_2 storage in the Qian-5 member.

6. Conclusions

The key findings of this study are:

(i) Regarding sedimentary facies, the reservoirs of saline aquifers in the Qian-5 member in the northeastern Ordos Basin comprise distributary channel sand bodies of deltaic plains. The study area hosts three NNE-extending distributary channels. The saline aquifers in the study area, located in deep, closed retention zones overall, have low-porosity and -permeability reservoirs and a hydrochemical type of Cl-Ca·Na.

(ii) The Qian-5 member in the study area contains three saline aquifer zones in Mahe in Yuyang, Jinjie-Yulin, and northern Jiaxian, which extend in an NNE direction along major channels. The saline aquifers in these zones generally have single-layer thicknesses of 3–8 m and average single-well cumulative thicknesses of generally 8–24 m. The Jinjie-Yulin saline aquifer zone is distributed the most widely, covering an area of 8929 km^2 and having an average saline aquifer thickness of 18 m.

(iii) The Qian-5 member in the northeastern Ordos Basin has a CO_2 technical control capacity of 119.25 × 10^6 t. The saline aquifer zones in Mahe in Yuyang, Jinjie-Yulin, and northern Jiaxian have storage capacities of 39.39 × 10^6 t, 73.34 × 10^6 t, and 6.52 × 10^4 t, respectively. The Jinjie-Yulin saline aquifer zone, whose storage capacity accounts for 64% of the total storage capacity of the member, has the highest potential for CO_2 storage.

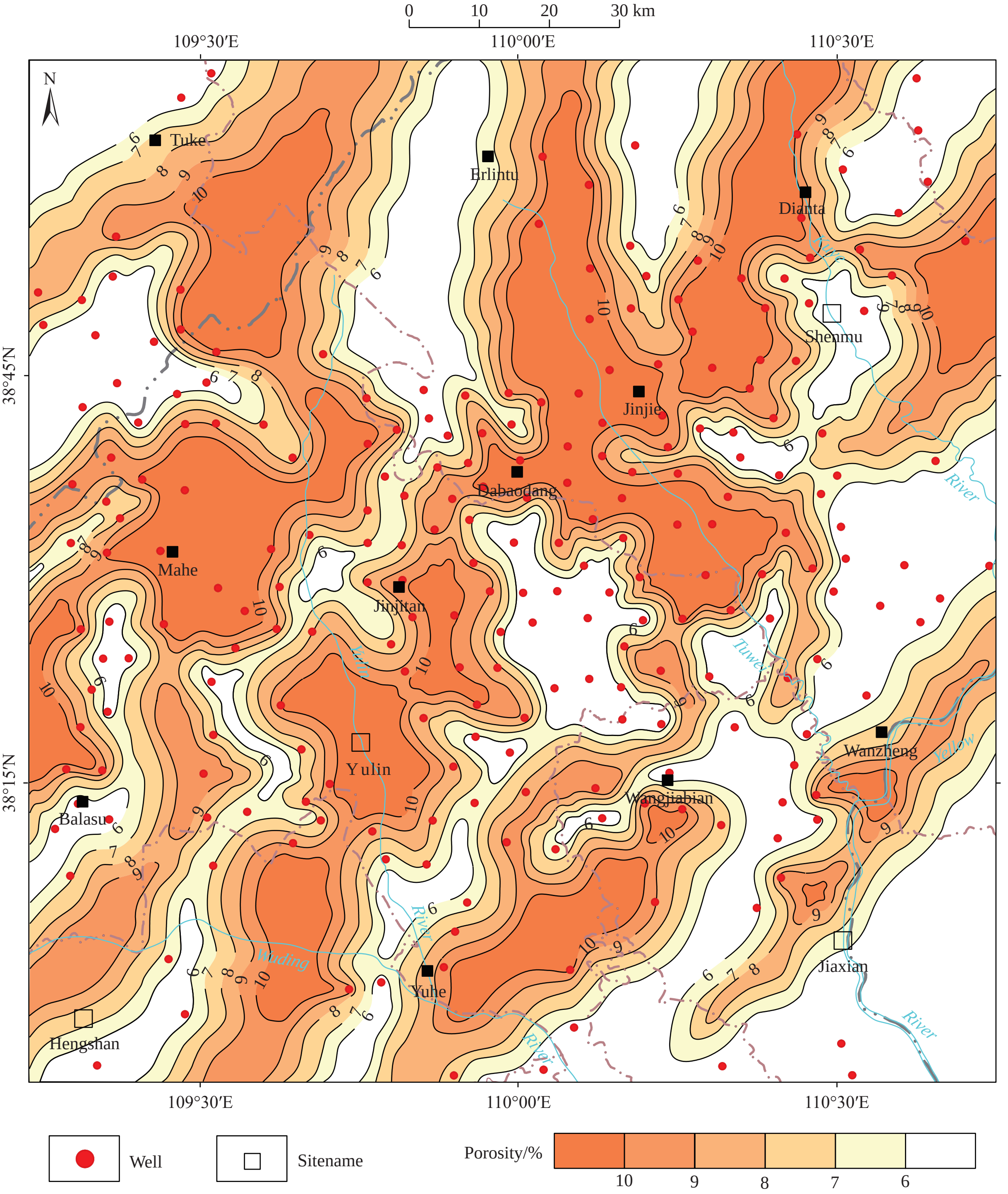

Fig. 14. Logging interpretation-derived porosities of the Qian-5 member in the northeastern Ordos Basin.

Table 2. CO_2 density of the Qian-5 member in the northeastern Ordos Basin and its calculation parameters.

Calculation unit	Formation depth/m	Pressure coefficient	Formation pressure (P) /Mpa	Geothermal gradient /°C/100 m	Formation temperature (T)/°C	CO_2 density(ρ) /kg·m^{-3}
Ⅰ	2612	0.765	19.60	2.75	88.83	531.26
Ⅱ	2506	0.765	18.81	2.8	87.17	515.05
Ⅲ	2262	0.765	16.98	2.85	81.47	485.41
Ⅳ	1741	0.765	13.07	2.85	66.62	437.77
Ⅴ	1661	0.765	12.47	2.95	66.00	408.17
Ⅵ	1510	0.765	11.33	2.95	61.55	368.62

Notes: pressure coefficients after Liu Z et al. (2012), geothermal gradients after Ren ZL et al. (2007), and CO_2 density calculation equation after Span R and Wagner W (1996).

Table 3. Recommended values of coefficients involved in the geological storage of CO_2 in clastic reservoirs in saline aquifers (after Goodman A et al., 2011).

Effective coefficient	$E_{An/At}$ (P_{10}/P_{90})	$E_{hn/hg}$ (P_{10}/P_{90})	$E_{e/tot}$ (P_{10}/P_{90})	E_v (P_{10}/P_{90})	E_d (P_{10}/P_{90})	E ($P_{10}/P_{50}/P_{90}$)
Value	0.2/0.8	0.21/0.76	0.64/0.77	0.16/0.39	0.35/0.76	1.2%/2.4%/2.8%

Table 4. Technical control capacities of CO_2 of the Qian-5 member in the northeastern Ordos Basin and their calculation parameters.

Calculation unit	Area/km^2	Porosity/%	Effective thickness of saline aquifers/h (m)	Well quantity	Well density (per km^2)	Regional storage capacity (× 10^6 t)	Saline-aquifer storage capacity (× 10^6 t)
Ⅰ	396	8.84	16.88	6	0.015	3.77	39.39
Ⅱ	4140	8.56	16.27	43	0.010	35.62	
Ⅲ	4191	8.61	19.66	68	0.016	41.78	73.34
Ⅳ	1369	8.78	16.67	23	0.017	10.53	
Ⅴ	3368	7.96	16.01	50	0.015	21.03	
Ⅵ	1507	6.55	14.94	12	0.008	6.52	6.52
Total	14970.99	/	/	202	/	119.25	119.25

CRediT authorship contribution statement

Yan Li, Peng Li, Hong-jun Qu and Gui-wen Wang conceived of the presented idea. Xiao-han Sun, Chang Ma and Tian-xing Yao carried out the experiment. All authors discussed the results and contributed to the final manuscript.

Declaration of competing interest

The authors declare no conflicts of interest.

Acknowledgement

This study was jointly funded by the Top 10 key scientific and technological projects of CHN Energy in 2021 entitled *Research and Demonstration of Technology* for *Carbon Dioxide Capture and Energy Recycling Utilization* (GJNYKJ [2021] No.128, No.: GJNY-21-51) and the Carbon Neutrality College (Yulin), Northwest University project entitled *Design and research of large-scale CCUS cluster construction in Yulin area, Shaanxi Province* (YL2022-38-01).

References

Bachu S. 2000. Sequestration of CO_2 in geological media: Criteria and approach for site selection in response to climate change. Energy Conversion and Management, 41(9), 953–970 . doi: 10.1016/s0196-8904(99)00149-1.

Bachu S. 2003. Screening and ranking of sedimentary basins for sequestration of CO_2 in geological media in response to climate change. Environmental Geology, 44(3), 277–289 . doi: 10.1007/s00254-003-0762-9.

Bachu S. 2008. CO_2 storage in geological media: Role, means, status and barriers to deployment. Progress in Energy and Combustion Science, 34(2), 254–273. doi: 10.1016/j.pecs.2007.10.001.

Bachu S. 2015. Review of CO_2 storage efficiency in deep saline aquifers. International Journal of Greenhouse Gas Control, 40(9), 188–202. doi: 10.1016/j.ijggc.2015.01.007.

Bachu S, Adams J. 2003. Sequestration of CO_2 in geological media in response to climate change: Capacity of deep saline aquifers to sequester CO_2 in solution. Energy Conversion and Management, 44(20), 3153–3175. doi: 10.1016/s0196-8904(03)00101-8.

Benson SM, Surles T. 2006. Carbon dioxide capture and storage: An overview with emphasis on capture and storage in deep geological formations. Proceedings of the IEEE, 94(10), 1795–1804 . doi: 10.1109/jproc.2006.883718.

Cao ML, Chen JP. 2022. Geological evaluation of CO_2 deep saline aquifer storage site selection. Acta Geologica Sinica, 96(5), 1868–1882 (in Chinese with English abstract).

Diao YJ. 2017. Study on the Researvoir Characterization and CO_2 Migration Underground in the Shenhua CCS Demonstration Project Site, China University of Mining and Technology, Ph. D thesis, 1–34 (in Chinese with English abstract).

Diao YJ, Ma X, Li XF, Zhang CL, Liu T. 2021. Study on the evaluation method of underground utilization space of CO_2 geological storage in saline aquifers. Geological Survey of China, 8, 87–91 (in Chinese with English abstract).

Diao YJ, Liu T, Wei N, Ma X, Jin XL, Fu L. 2023. Classification and assessment methodology of CO_2 geological storage in deep saline aquifers. Geology in China, 50(3), 943-951 (in Chinese with English abstract). doi: 10.12029/gc20221030001.

Goodman A, Hakala A, Bromhal G, Deel D, Rodostab T, Frailey S, Small M, Allen D, Romanov V, Fazio J, Huerta N, Mcintyre D, Kutchko B, Guthrie G. 2011. U. S. DOE methodology for the development of geologic storage potential for carbon dioxide at the national and regional scale. International Journal of Greenhouse Gas Control, 5(4), 952–965. doi: 10.1016/j.ijggc.2011.03.010.

Guo JQ, Wen DG, Zhang SQ, Xu TF, Li XF, Diao YJ, Jia XF. 2015. Evaluation and demonstration project of carbon dioxide geological storage potential in China. Geological Survey of China, 2(4), 36–46 (in Chinese with English abstract).

Guo YQ, Li WH, Guo BC, Zhang Q, Chen Q, Wang RG, Liu X, Ma Y, Li ZC, Zhang MT, Li BQ. 2019. Sedimentary system and paleogeographic evolution of Ordos Basin. Paleogeography, 21(2), 293–318 (in Chinese with English abstract).

He B, Xu TF, Yuan YL, Tian HL, Hou ZY, Wang FG. 2016. An analysis of the influence factors on CO_2 injection capacity in a deep saline formation: A case study of Shiqianfeng Group in the Erdos Basin. Hydrogeology & Engineering Geology, 43(1), 136–142 (in Chinese with English abstract).

Hou GC, Zhang MS, Liu F, Wang YH, Liang YP, Tao ZP, Zhao ZH, Hu FS, Su XS, Lv Y, Xie Y, Wang WK, Wang XY, Yang YY, Lu Q, Jiao YQ, Yang YC, Cui XD, Ma JL, Yin LH. 2008. Groundwater exploration in Ordos Basin. Geological Publishing House, Beijing, 66–80.

Jia LX. 2021. Earth sciences critical to achieving net zero emission of greenhouse gas in the context of carbon neutrality. Geology in China, 48(4), 1304 (in Chinese with English abstract).

Kumar A, Ozah R, Noh M, Pope GA, Bryant S, Sepehmoori K, Lake

LW. 2004. Reservoir simulation of CO_2 storage in deep saline aquifers. SPE Journal, 10(3), 336–348. doi: 10.2118/89343-ms.

Li FC, Zhang Y, Zhang XJ, Zheng CY, Li XF, Hu LS, Peng HM. 2014. Study on the suitability evaluation method of CO_2 geological storage in deep saline aquifer. Journal of Glaciology and Geocryology, 36, 649–660 (in Chinese with English abstract).

Lindeberg E, Wessel-Berg D. 1997. Vertical convection in an aquifer column under a gas cap of CO_2. Energy Conversion and Management, 38(SUPP.1), 229–234 . doi: 10.1016/s0196-8904(96) 00274-9.

Liu CY, Zhao HG, Gui XJ, Yue LP, Zhao JF, Wang JQ. 2006. Spatial-temporal coordinates of evolution-transformation of Ordos Basin and its response to hydrocarbon accumulation (mineralization). Acta Geologica Sinica, 80(5), 617–638 (in Chinese with English abstract).

Liu SX, Peng B, Liu Q, Fan C. 2019. Economic-related CO_2 emissions analysis of Ordos Basin based on a refined STIRPAT model. Greenhouse Gases Science and Technology, 9(5), 1064–1080 . doi: 10.1002/ghg.1920.

Liu Z, Zhu WQ, Sun Q, Jin B, Xu XM, Zhang HF. 2012. Geothermal-geopressure system of petroliferous basins in China. Acta Petrolei Sinica, 33(1), 1–17 (in Chinese with English abstract). doi: 10.1038/aps.2011.197.

Ma DY, Chen YH, Wang YB, Guo MQ, Qu L, Zhao JZ, Wu HY. 2021. Evaluation of sealing performance of upper Paleozoic caprock in eastern Ordos Basin. Natural Gas Geosciences, 32(11), 1673–1684 (in Chinese with English abstract).

Ma JF, Li L, Wang HF, Du Y, Ma JJ, Zhang XL, Wang ZL. 2022. Carbon capture and storage: History and the road ahead. Engineering, 14(7), 33–43. doi: 10.1016/j.eng.2021.11.024.

Ma X, Wen DG, Yang GD, Li XF, Diao YJ, Dong HH, Cao W, Yin SG, Zhang YM. 2021. Potential assessment of CO_2 geological storage based on injection scenario simulation: A case study in eastern Junggar Basin. Journal of Groundwater Science and Engineering, 9(4), 279–291. doi: 10.19637/j.cnki.2305-7068.2021.04.002.

Nan D, Jin ZQ, Wang HP, Lv ZW, Wang B. 2022. Research progress of logging data evaluation of CO_2 geological storage in saline aquifer. Well Logging Technology, 46(3), 241–250 (in Chinese with English abstract).

Popova OH, Small MJ, Mccoy ST, Thomas AC, Karimi B, Goodman A, Carter KM. 2012. Comparative analysis of carbon dioxide storage resource assessment methodologies. Environmental Geosciences, 3(3), 105–124. doi: 10.1036/eg.06011212002.

Ren ZL, Zhang S, Gao SL, Cui JP, Xiao YY, Xiao H. 2007. Tectono-thermal evolution history of Ordos Basin and its significance for hydrocarbon accumulation and mineralization. Chinese Science (Series D: Earth Science), 37(S1), 23–32 (in Chinese with English abstract).

Song TJ, Wan YY, Zhang WQ, Rao WD, Meng JY, Fan JJ, Gao RM. 2017. Applicability evaluation of CO_2 geological storage in Songliao Basin based on grey correlation analysis. Geological Bulletin of China, 36(10), 1874–1883 (in Chinese with English abstract).

Span R, Wagner W. 1996. A new equation of state for carbon dioxide covering the fluid region from the triple-point temperature to 1100 K at pressures up to 800 MPa. Journal of Physical and Chemical Reference Data, 25(6), 1509–1596. doi: 10.1063/1.555991.

Sun TM, Liu SQ, Wang T. 2021. Research progress on potential evaluation of carbon dioxide geological storage in China. Coal Science and Technology, 49, 10–20 (in Chinese with English abstract).

USDOE. 2006. Carbon sequestration atlas of the United States and Canada: Appendix A-Methodology for development of carbon sequestration capacity estimates, 71–85.

Wan YY. 2012. Migration and Transformation Characteristics of CO_2 in CO_2 Geological Storage in Saline Aquifers of Shiqianfeng Formation in Ordos Basin. Changchun, Jilin University, Ph. D thesis, 1–79 (in Chinese with English abstract).

Wang RG. 2016. Sedimentary facies analysis of Qian 5 Member of Shiqianfeng Formation in Yanchang exploration area, Ordos Basin. Petroleum Geology and Engineering, 30(06), 1–4+126 (in Chinese with English abstract).

Wang ZJ, Tang X, Jing TY, You MX, Zhang JC, Li Z, Zhou J. 2022. Million-ton CO_2 geological storage site selection strategy in China. Geoscience, 36(5), 1414–1431 (in Chinese with English abstract).

Yang GD. 2015. Research on Geological Storage Mechanism of Carbon Dioxide in Ordos Basin. Wuhan, China University of Geosciences, Ph. D thesis, 1–80 (in Chinese with English abstract).

Yang YZ, Shen PP, Song XM, Yang SY, Hu YL. 2009. Greenhouse gas geo-sequestration mechanism and capacity evaluation in aquifer. Journal of Jilin University(Earth Science Edition), 39(4), 743–748 (in Chinese with English abstract).

Zhang DF, Li CS, Liu WX, Ma GW, Li WH, Lu ZX. 2021. Sedimentary characteristics of Upper Permian in Ordos Basin and its surrounding areas. Journal of Paleogeography, 23(1), 93–104 (in Chinese with English abstract).